Available online at www.sciencedirect.com
ScienceDirect
Materials Research Bulletin 41 (2006) 2198–2203
Materials Research Bulletin
www.elsevier.com/locate/matresbu

The strain reduction and quality improvement in ZnO film by a 30° in-plane rotation with respect to the Al_2O_3 substrate

Shengqiang Zhou [a,*], M.F. Wu [a], S.D. Yao [a,**], Y.M. Lu [b], Y.C. Liu [b]

[a] *Department of Technical Physics, School of Physics, Peking University, Beijing 100871, PR China*
[b] *Open Laboratory of Excited State Processes, Chinese Academy of Sciences, Changchun Institute of Optics, Fine Mechanics and Physics, 1-Yan An Road, Changchun 130021, PR China*

Received 20 September 2005; received in revised form 20 April 2006; accepted 25 April 2006
Available online 15 May 2006

Abstract

The in-plane orientation of epitaxial ZnO thin film on Al_2O_3(0 0 0 1) was determined by azimuthal scan of X-ray diffraction. Comprehensive structural characterizations, including the lattice strain in perpendicular direction, the defect density, were obtained from high resolution X-ray diffraction. It's found that a 30° rotation in ZnO against Al_2O_3, resulting in ZnO$\langle 1\ 1\ \underline{2}\ 0\rangle$// $Al_2O_3\langle 1\ 0\ \underline{1}\ 0\rangle$, can efficiently reduce the strain and defects in ZnO layer. Consequently, the optical property is significantly improved.

Keywords: B. Epitaxial growth; C. X-ray diffraction; D. Crystal structure

1. Introduction

Zinc oxide (ZnO) is a II–VI semiconductor with properties similar to GaN [1]. Like GaN, it has a direct band gap in the ultraviolet range (≈3.3 eV) at room temperature and a stable wurtzite structure. ZnO is therefore another candidate for optoelectronic applications in the short wavelength range [2–4]. What's more, ZnO has a higher exciton binding energy of about 60 meV (28 meV for GaN), which would allow the formation of excitons and efficient excitonic emission even at room temperature [5,6]. Up to date, the epitaxial ZnO films have been successfully grown on sapphire substrate by molecular beam epitaxy [6,7], plasma enhanced chemical vapor deposition [8], and metal-organic chemical vapor deposition [9,10]. Different growth condition and substrate process result in a different in-plane orientation between ZnO and Al_2O_3 [11,12]. The polarity of ZnO films with different in-plane orientation has been studied using coaxial impact collision ion scattering spectroscopy [11,12]. Unfortunately as we know by far, no systematic work on the behaviours of lattice strain and defects with respect to the in-plane orientationship between ZnO and Al_2O_3 has been reported. In the work, the lattice strain, the mosaic structures, and the photoluminescence are comprehensively compared in epitaxial ZnO films with different in-plane orientation respect to the substrates of Al_2O_3.

* Corresponding author. Tel.: +49 351 260 2065; fax: +49 351 260 3285.
** Corresponding author.
E-mail addresses: s.zhou@fz-rossendorf.de (S. Zhou), sdyao@pku.edu.cn (S.D. Yao).

0025-5408/$ – see front matter © 2006 Elsevier Ltd. All rights reserved.
doi:10.1016/j.materresbull.2006.04.032

2. Experiment

The ZnO samples were prepared on Al_2O_3(0 0 0 1) substrate by plasma enhanced chemical vapor deposition. X-ray diffraction measurements were carried out on a Bruker D8 diffractometer system, using four Ge(2 2 0) as the monochromator. The X-ray source is Cu kα1 with a wavelength of 0.154056 nm. The full width at half maximum (FWHM) of the rocking curve of Al_2O_3(0 0 0 6) is 0.006° that can roughly be taken as the set-up resolution. The optical properties of films were characterized by photoluminescence (PL) spectroscopy using the 325 nm line of a He–Cd laser.

3. Results and discussion

3.1. Orientation between ZnO and Al_2O_3

The in-plane orientation of ZnO film respect to Al_2O_3 substrate was determined by the ϕ-scan of X-ray diffraction. Fig. 1. shows the ϕ-scan of ZnO(1 0 $\underline{1}$ 1) and Al_2O_3(1 1 $\underline{2}$ 3). The Al_2O_3(1 1 $\underline{2}$ 3) diffraction reveals a six-fold symmetry as expected. For sample A, ZnO(1 0 $\underline{1}$ 1) diffraction reveals a six-fold symmetry with an azimuthal shift of 30° respecting to the Al_2O_3(1 1 $\underline{2}$ 3) planes. Therefore in sample A, the in-plane orientation is ZnO⟨1 0 $\underline{1}$ 0⟩//Al_2O_3⟨1 0 $\underline{1}$ 0⟩. For sample B, ZnO(1 0 $\underline{1}$ 1) diffraction reveals a six-fold symmetry at the same azimuthal positions as the Al_2O_3(1 1 $\underline{2}$ 3) planes, that results in the in-plane orientationship of ZnO⟨1 1 $\underline{2}$ 0⟩//Al_2O_3⟨1 0 $\underline{1}$ 0⟩. While in sample C, the diffraction of ZnO(1 0 $\underline{1}$ 1) displays a 12-fold symmetry, indicates the above two phases coexist. Table 1 shows the lattice constants and corresponding planar spacings of bulk ZnO and Al_2O_3. The lattice mismatch f, can be calculated as $f = (d_{layer} - d_{sub})/d_{sub}$, where d_{layer} and d_{sub} are the planar spacing for ZnO and Al_2O_3, respectively. For sample B, with the 30° rotation of the ZnO epilayer against the Al_2O_3 substrate, the lattice mismatch is reduced from around −32% to +18%. Accompanying the lattice mismatch reduction, the lattice strain and the defects are expected to reduce efficiently, consequently the enhancement of optical properties. From the pattern of ϕ-scan, sample B already shows better crystalline quality than sample A and C. In the following, High resolution X-ray diffraction is used to determine the lattice constant, and to evaluate the defect density. Photoluminescence is used to compare the optical properties.

3.2. Lattice parameters and elastic strain

The lattice constant of ZnO epilayer in *c*-direction was calculated from the peak of ZnO (0 0 0 2) diffraction. Fig. 2 representatively shows the $2\theta - \theta$ scan of ZnO(0 0 0 2) and Al_2O_3(0 0 0 6) for sample B, which indicates that the wurtzite ZnO is formed with *c*-axis oriented on Al_2O_3, and no other growth direction is detectable. The inset shows the

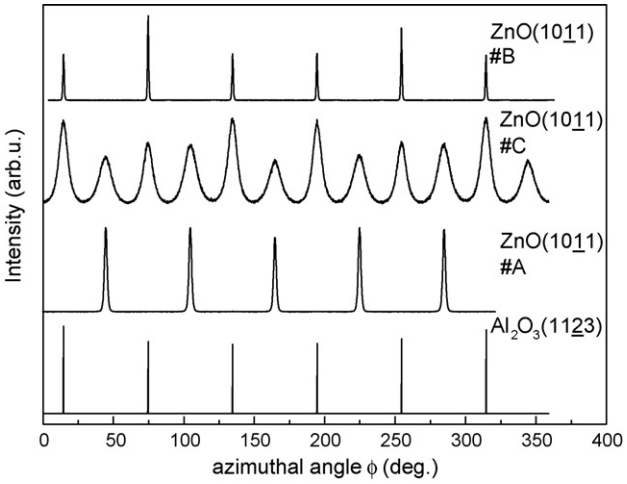

Fig. 1. XRD Φ-scans of ZnO(1 0 $\underline{1}$ 1) and substrate Al_2O_3(1 1 $\underline{2}$ 3) of sample A, B, and C. In sample C, two phases of ZnO⟨1 0 $\underline{1}$ 0⟩//Al_2O_3⟨1 0 $\underline{1}$ 0⟩, and ZnO⟨1 1 $\underline{2}$ 0⟩//Al_2O_3⟨1 0 $\underline{1}$ 0⟩ coexist.

Table 1
Lattice parameter and interplanar spacing for ZnO and Al_2O_3 (in nm)

Material	ZnO	Al_2O_3
Lattice parameter		
a	0.3250	0.4758
c	0.5205	0.12991
Interplanar spacing		
(1 0 $\underline{1}$ 0)	0.2815	0.4120
(1 1 $\underline{2}$ 0)	0.1625	0.2379

ZnO(0 0 0 2) peak for different sample. Taking the Al_2O_3(0 0 0 6) peak as the reference, the Bragg angle of ZnO(0 0 0 2) can be accurately determined as following, $\theta_{ZnO(0002)} = \theta_{Al_2O_3(0006)} - \Delta\theta$, $\theta_{Al_2O_3(0006)} = 20.838^\circ$ is the theoretical value of the Al_2O_3(0 0 0 6) Bragg angle, and $\Delta\theta$ is the Bragg angle difference between ZnO(0 0 0 2) peak and Al_2O_3(0 0 0 6) peak in experimental spectrum. According to the Bragg equation, $2d \sin\theta = \lambda$, where d is the lattice spacing, θ is the Bragg angle and λ is the incident X-ray wavelength, the c lattice constant for ZnO can be determined.

The strain in perpendicular direction can be calculated by the following equation, $e^{\perp} = ((c - c_{bulk})/c_{bulk}) \times 100\%$, where c_{bulk} is the lattice constant of bulk ZnO. The calculated lattice constants and elastic strains are shown in Fig. 3. In perpendicular direction, the lattices of sample A and C are compressed, while sample B is tensile. Therefore, by concerning the theory of elastic strain for hexagonal structure, the lattices in parallel direction are tensile and compressive for sample A and B, respectively, which is agreeable with the lattice mismatch. What's more, the strain value in sample B is smaller than that in sample A, which benefits from the smaller lattice mismatch.

3.3. Mosaic spread

Additionally, X-ray diffraction can be used to detect the tilt and twist mosaic spread of the film induced by the presence of dislocation, and therefore indirectly give the density of dislocations. Several approaches are proposed to determine the in-plane mosaic structure, the so-called twist angle [13–15]. In this work, the approach combining ϕ-scan and ω-scan of asymmetric planes was adopted [15]. For sample A and B, the rocking curves and ϕ-scans of a series of planes of (1 0 $\underline{1}$ 1), (1 0 $\underline{1}$ 2) (1 0 $\underline{1}$ 3) and (1 0 $\underline{1}$ 5), were carried out at symmetric skew mode. Fig. 4a shows the representative ϕ-scan and ω-scan. The FWHM of X-ray diffraction peak was determined by fitting to a Pseudo-Voight function. Fig. 4b shows the dependence of FWHM on the lattice inclination angle. FWHMs of ϕ-scans decrease

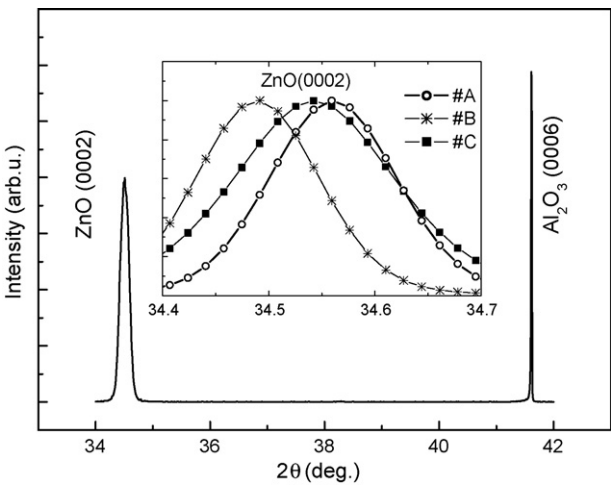

Fig. 2. Symmetric $2\theta - \theta$ scan of the ZnO (0 0 0 2) and Al_2O_3 (0 0 0 6) diffraction (sample B). Inset shows the ZnO(0 0 0 2) peaks where the peak position is shifted for different sample.

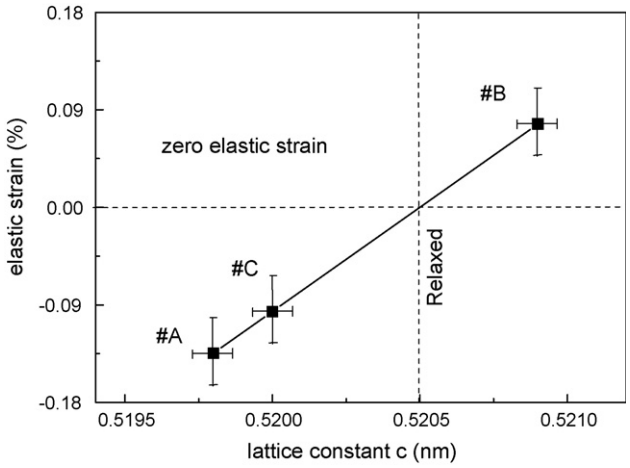

Fig. 3. Residual elastic strain (%) in perpendicular direction of samples A, B, and C.

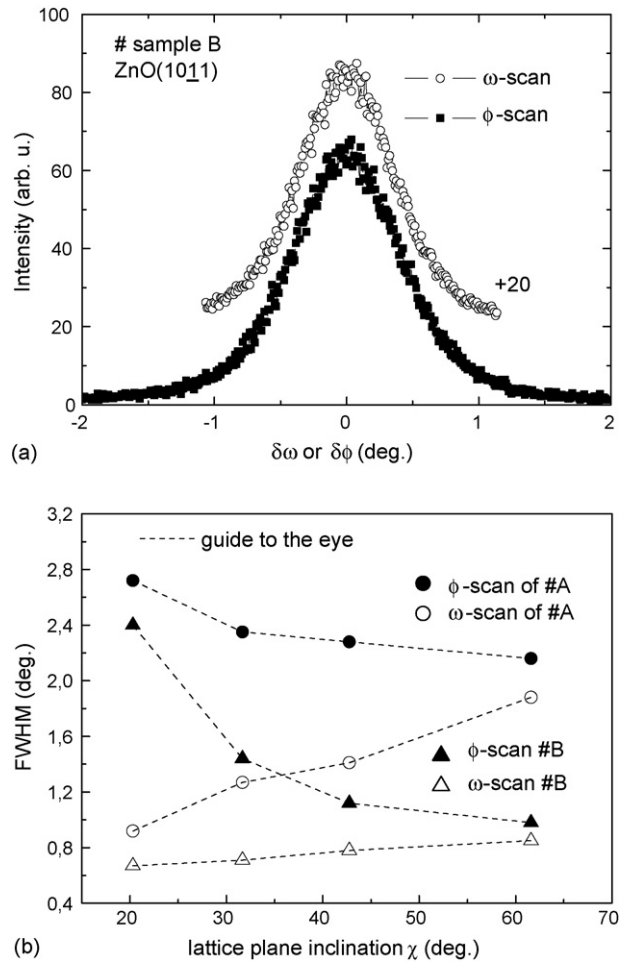

Fig. 4. (a) Representative Φ-scan and ω-scan. (b) FWHM of Φ-scan and ω-scan in skew symmetric mode as a function of the lattice inclination angle. The lattice plane is (1 0 $\underline{1}$ l) with $l = 5$, 3, 2, and 1, respectively, with increasing inclination angle.

Table 2
Defect density in ZnO sample

Sample	Tilt spread (°)	D_{screw} (cm^{-2})	Twist spread (°)	D_{edge} (cm^{-2})	D_{total} (cm^{-2})
A	0.55	3.8×10^9	2.1	1.4×10^{11}	1.4×10^{11}
B	0.66	5.4×10^9	0.92	2.7×10^{10}	2.8×10^{10}

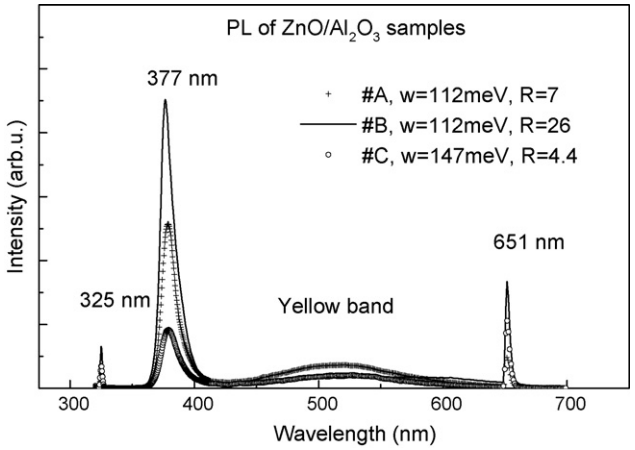

Fig. 5. Room temperature PL spectra of ZnO samples. R is intensity ratio of the near-band-gap to the yellow band, and w is the FWHM of near-band-gap emission.

with the increment of χ angle, while those of ω-scans increase. The average of the FWHMs of (1 0 $\underline{1}$ 1) ϕ-scan and ω-scan is taken as an approximation of the twist angle. According to Ref. [16], the rocking curve of (0 0 0 2) can be related to the density of screw threading dislocations, while the twist angle corresponds to the density of edge threading dislocations. The dislocation density of ZnO epilayer can be estimated by the following equations [17]. $D_{screw} = \beta_{tilt}^2/9b_{screw}^2$, $D_{edge} = \beta_{twist}^2/9b_{edge}^2$, and total dislocation density $D = D_{screw} + D_{edge}$ where β is the tilt or twist spread and b is the Burger vector length (for ZnO $b_{screw} = \langle 0\,0\,0\,1\rangle = 0.5205$ nm, and $b_{edge} = (1/3)\langle 1\,1\,\underline{2}\,0\rangle = 0.3250$ nm). The calculated dislocation density is listed in Table 2. For sample C, the coexisting of two phase heavily degrades the crystalline quality, so that the mentioned above measurements cannot be reached. In sample B, the in-plane defects are significantly reduced compared with sample A. Noting that the rocking curve of (0 0 0 2) of sample A is even thinner than that of sample B, it can be explained by considering that rocking curve of (0002) cannot be used to evaluate the material quality with respect to the optical and electrical properties [16,18].

3.4. Photoluminescence

In the photoluminescence spectra of GaN epilayer on Al_2O_3, the parasitic yellow band (around 500–600 nm) is attributed to the dislocation defects [19–21]. The ratio of the peak intensities of the bandgap-to-yellow luminescence is taken as a merit of the material quality. Fig. 5 shows the photoluminescence from the ZnO epilayer at room temperature. The dominant peaks pointing at 377 nm (3.29 eV) correspond to the near-band-gap emission in a wurtzite ZnO crystal. The intensity from sample B is roughly twice of sample A, and five times of sample C. The very broad peak around 530 nm (2.35 eV) is the so-called yellow band. The intensity ratios of the near-band-gap to the yellow band are approximately 7, 26 and 4.4 for sample A, B and C, respectively, which strongly indicates sample B has the best optical quality.

4. Concolusion

In a conclusion, ZnO thin films were epitaxially grown on Al_2O_3(0001). The in-plane orientation between ZnO and Al_2O_3 can be ZnO$\langle 1\,0\,\underline{1}\,0\rangle$//$Al_2O_3\langle 1\,0\,\underline{1}\,0\rangle$, or ZnO$\langle 1\,1\,\underline{2}\,0\rangle$//$Al_2O_3\langle 1\,0\,\underline{1}\,0\rangle$, or the above two phases coexisting. In-

plane orientation of ZnO$\langle 1\ 1\ \underline{2}\ 0\rangle$//$Al_2O_3\langle 1\ 0\ \underline{1}\ 0\rangle$ results in a 30° rotation of the ZnO epilayer against the Al_2O_3 substrate, which reduces the lattice mismatch from −32% to 18%. As a beneficial result, the residual strain and the structural defects are greatly reduced. Consequently, the optical quality is significantly enhanced.

Acknowledgement

This work was partially supported by National Natural Science Foundation under the grant NO. 10375004.

References

[1] R.D. Vispute, V. Talyansky, S. Choopun, R.P. Sharma, T. Venkatesan, M. He, X. Tang, J.B. Halpern, M.G. Spencer, Y.X. Li, L.G. Salamanca-Riba, A.A. Iliadis, K.A. Jones, Appl. Phys. Lett. 73 (1998) 348.
[2] Y.F. Chen, D.M. Bagnall, T. Yao, Mat. Sci. Eng. B 75 (2000) 190.
[3] D.C. Look, Mat. Sci. Eng. B 80 (2001) 383.
[4] A. Ohtomo, H. Kawasaki, Y. Sakurai, I. Ohkubo, R. Shiroki, Y. Yoshida, T. Yasuda, Y. Segawa, H. Koinuma, Mat. Sci. Eng. B 56 (1998) 263.
[5] D.M. Bagnall, Y.F. Chen, Z. Zhu, T. Yao, S. Koyama, M.Y. Shen, T. Goto, Appl. Phys. Lett. 70 (1997) 2230.
[6] Y. Segawa, A. Ohtomo, M. Kawasaki, H. Koinuma, Z.K. Tang, P. Yu, G.K.L. Wong, Phys. Status Solidi B 202 (1997) 669.
[7] Y.F. Chen, D.M. Bagnall, H. Koh, K. Park, K. Hiraga, Z. Zhu, T. Yao, J. Appl. Phys. 84 (1998) 3912.
[8] B.S. Li, Y.C. Liu, Z.S. Chu, D.Z. Shen, Y.M. Lu, J.Y. Zhang, X.W. Fan, J. Appl. Phys. 91 (2002) 501.
[9] J.D. Ye, S.L. Gu, S.M. Zhu, T. Chen, L.Q. Hu, F. Qin, R. Zhang, Y. Shi, Y.D. Zheng, J. Cryst. Growth 243 (2002) 151.
[10] S. Muthukumar, J. Zhong, Y. Chen, Y. Lu, T. Siegrist, Appl. Phys. Lett. 82 (2003) 742.
[11] I. Ohkubo, A. Ohtomo, T. Ohnishi, Y. Mastumoto, H. Koinuma, M. Kawasaki, Surf. Sci. 443 (1999) L1043.
[12] B.P. Zhang, L. Manh, K. Wakatsuki, K. Tamura, T. Ohnishi, M. Lippmaa, N. Usami, M. Kawasaki, H. Koinuma, Y. Segawa, Jpn. J. Appl. Phys. 42 (2003) L264.
[13] V. Srikant, J.S. Speck, D.R. Clarke, J. Appl. Phys. 82 (1997) 4286.
[14] H. Heinke, V. Kirchner, S. Einfeldt, D. Hommel, Appl. Phys. Lett. 77 (2000) 2145.
[15] X.H. Zheng, H. Chen, Z.B. Yan, Y.J. Han, H.B. Yu, D.S. Li, Q. Huang, J.M. Zhou, J. Cryst. Growth 255 (2003) 63.
[16] B. Heying, X.H. Wu, S. Keller, Y. Li, D. kapolnek, B.P. Keller, S.P. Debbaars, J.S. Speck, Appl. Phys. Lett. 68 (1996) 643.
[17] R. Gay, P.B. Hirsch, A. Kelly, Acta Metall. 1 (1953) 315.
[18] Q. Zhu, A. Botchkarev, W. Kim, O. Aktas, A. Salvador, B. Sverdlov, H. Morkoc, S.C.Y. Tsen, D.J. Smith, Appl. Phys. Lett. 68 (1996) 1141.
[19] F.A. Ponce, D.P. Bour, W. Gotz, P.J. Wright, Appl. Phys. Lett. 68 (1996) 57.
[20] D. Cherns, S.J. Henley, F.A. Ponce, Appl. Phys. Lett. 78 (2001) 2691.
[21] Y. Cho, H.M. Kim, T.W. Kang, J.J. Song, W. Yang, Appl. Phys. Lett. 80 (2002) 1141.